

Current Estimation and Remote Temperature Monitoring System for Low Power Digitally Controlled DC-DC SMPS

Zdravko Lukić, Andrija Stupar, and Aleksandar Prodić

Laboratory for Low-Power Management and Integrated SMPS
ECE Department, University of Toronto
10 King's College Road
Toronto, ON M5S 3G4, CANADA
e-mail: prodic@power.ele.utoronto.ca

Dimitry Goder

Exar Corporation
48720 Kato Road
Fremont, CA 94538
USA

Abstract - This paper describes a simple adaptive digital system that can accurately estimate steady-state inductor current and, at the same time, provide remote temperature monitoring of power switches in low-power digitally controlled dc-dc converters. The system is well-suited for on-chip implementation. It provides a solution for combining a digital controller, current estimator and remote temperature monitor on a single integrated circuit. To estimate the current and temperature, the estimator utilizes inherently available information about the duty ratio and performs auto-calibration through the utilization of a current sink. During regular converter operation, a known load current step is introduced and the inductor current and a dc resistance R_{eq} emulating converter losses are calculated from the resulting increase in the duty ratio control variable. Then, based on the obtained resistance value, the temperature of the switching components is found. The effectiveness of the estimator is demonstrated on a digitally-controlled 1.5 V, 15 W buck converter operating at 500 kHz switching frequency.

I. INTRODUCTION

In low-power switch-mode power supplies (SMPS) information about steady state inductor current and the temperature of switching components can be used for improving power processing efficiency, dynamic response, and system reliability.

A. Current sensing

To extend the battery life of portable systems, multimode operation can be performed based on the inductor current. Examples of this include on-line switching between pulse-width and pulse-frequency modes of operation [1],[2], dynamic sizing of power switches [3], and gate-drive circuit adjustments [3].

The practical implementation of accurate current sensing has proven to be a challenging task in cost sensitive low-power SMPS [4],[5], which preferably have several functional blocks integrated on a single IC. Conventional voltage-drop based methods [6-10] usually require a fairly complex high gain-bandwidth amplifier or a lossy sensing resistor. In addition, the methods are not well-suited for on-chip integration with emerging digital controllers implemented in the latest CMOS technologies. The very low supply voltage severely limits the number of analog blocks that can be implemented, preventing

This work of Laboratory for Low-Power Management and Integrated SMPS is sponsored by Exar Corporation, Fremont, CA, USA.

current amplifiers from being integrated with the rest of the controller. As a result, costly multi-chip solutions increasing the system size and reducing reliability are required. Alternative methods, based on current estimation [11-16], potentially offer single chip solutions but often suffer from poor accuracy [17].

B. Temperature monitoring

Dedicated temperature sensors are placed next to the power switches as parts of the over-temperature protection system. They send information to the thermal protection circuit of the controller, which, in the case of overheating, shuts down the SMPS. Again, the implementation of such a system requires a multi-chip solution, not suitable for low-power systems. Hence, even though very useful, the temperature protection of switching components is often not applied.

C. Digital Current and Temperature Estimator

Fig.1 shows a combined current and temperature estimator

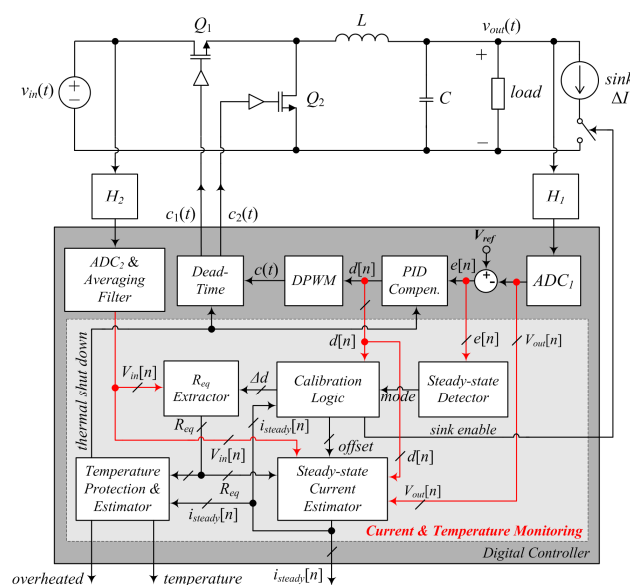


Fig. 1. A digitally controlled buck converter with current estimation and temperature protection system.

that is suitable for a single chip integration with modern low-power digital controllers. The new solution introduced here is a modification of a duty-ratio based current estimator [18], which, unlike the original solution, has high accuracy and, at the same time, can estimate the temperature of switching components. As shown in Fig.1, the estimator is designed to operate with conventional digital voltage mode pulse-width modulation controllers and does not require any modification of the basic controller circuit. Compared to the digital current estimator based on a self-tunable digital filter [19], this solution is much simpler for implementation since it utilizes simpler algorithm and requires adjustment of a smaller number of parameters. The simplicity comes at the price of a slower average current estimation.

In the following section, the duty ratio based estimation method is reviewed and the operation of the new system described. Section III addresses practical implementation challenges such as the influence of the non-overlapping circuit and other converter losses affecting the system accuracy and shows a solution for them. In the last section, we show experimental results obtained with a digitally-controlled buck converter prototype.

II. PRINCIPLE OF OPERATION

The duty-ratio based current estimator [18] calculates the dc value of the inductor/load current from a discrepancy between the ideal and actual duty ratio value in closed loop converter operation. It relies on the fact that, due to converter losses, actual duty ratio is larger than the ideal. The difference is proportional to the product of the load current and the emulated resistance that models total converter losses.

For example, for the buck converter of Fig. 1, a simplified dc equivalent model emulating losses can be derived as shown in Fig. 2. The steady-state output current I_{steady} of the model can be calculated as:

$$I_{steady} = \frac{D \cdot V_{in} - V_{out}}{R_{eq}}, \quad (1)$$

$$I_{steady} = \frac{D \cdot V_{in} - V_{out}}{D \cdot R_{ds_on1} + (1-D) \cdot R_{ds_on2} + R_L}, \quad (2)$$

where D stands for steady-state duty ratio, V_{in} and V_{out} for the input and output voltage, and R_{eq} is an equivalent resistance. The equivalent resistance is the sum of the MOSFET on-resistances $R_{ds_on1,2}$ and other losses R_{loss} , modeling inductor and switching losses [20]. Since, in a digital loop, D and V_{out} are readily available, by sampling the input voltage V_{in} and knowing R_{eq} the steady value of the output current can be easily estimated.

However, in practice, R_{eq} varies significantly with temperature, gate driver supply voltage, output load, and depends on non-overlapping transistor times. All of these significantly affect the estimation accuracy and make the conventional duty ratio based method impractical for most

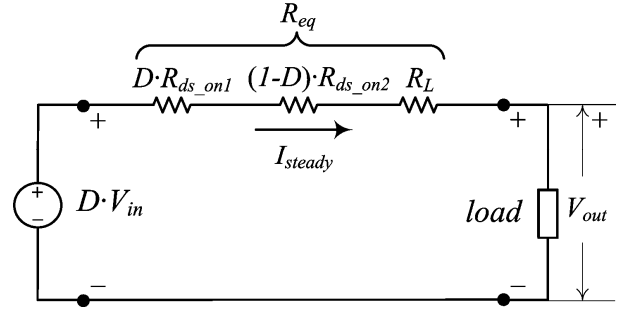


Fig. 2. A steady-state equivalent model of a buck converter

applications. To improve the accuracy and, at the same time, extract information about the temperature of components, in this implementation, a small current load, i.e. current sink, is connected to the output, as shown in Figs.1 and 3. The basic idea is to periodically increase the load current by a known current step ΔI and calibrate the estimator accordingly. The calibration technique is similar to that presented in [13] where a known current is injected to the inductor before the start-up. However, the limitation of the previous method is that during regular converter operation, it cannot be used since a path for the injected current is not available.

The system of Fig.1 performs the calibration and temperature estimation as follows. First, through the current sink, shown in Fig. 3, a current step of ΔI is introduced. As a consequence, the PID compensator increases the duty ratio control variable $d[n]$ to keep the output voltage $v_{out}(t)$ regulated. The calibration logic then calculates the difference Δd between steady-state duty ratio values before and after the sink is enabled. This difference is then passed to R_{eq} -Extractor that calculates the actual value of the equivalent resistance R_{eq} as:

$$R_{eq} = \frac{\Delta d \cdot V_{in}}{\Delta I}, \quad (4)$$

and updates the current estimation algorithm (1) implemented with the block named steady-state current estimator.

The extracted value of R_{eq} now can be used for the temperature monitoring of the power switches and overheating protection. As shown in Fig.4, R_{eq} depends on the temperature, meaning that, for a given operating condition, the temperature of the component can be found from R_{eq} and the load value only.

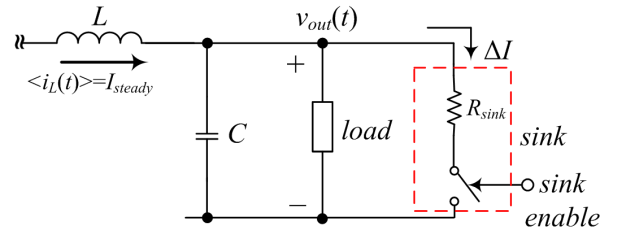


Fig. 3. Practical implementation of the current sink used for R_{eq} calibration.

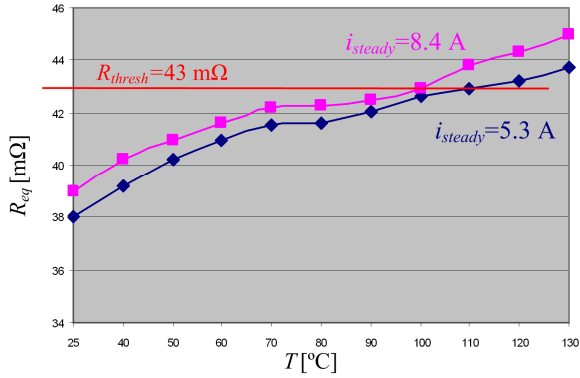


Fig. 4. Change of R_{eq} due to the ambient temperature for two different output load conditions

As it will be shown later, a fairly accurate estimate of the temperature can be obtained, by using a look up table with pre-stored temperatures for a range of R_{eq} and the load current values. In the diagram of Fig. 1, the look-up table is a part of the *temperature protection and estimator* block. If an overly high temperature of the components is detected, the block shuts down the switches and also sends an external overheat signal.

III. PRACTICAL IMPLEMENTATION

In practice, the accuracy of this method is significantly affected by the operation of dead-time (non-overlapping) circuit, and the input voltage deviations, caused by switching action of the converter.

The dead-time circuit makes the actual duty ratio value smaller than $d[n]$ causing a positive offset in the current estimation. The estimated current is larger than the true value by:

$$\Delta i_{steady} = \frac{\Delta d_{dt} \cdot V_{in}}{R_{eq}} \quad (5)$$

To compensate for this, during the converter start-up, the output load is disconnected and an initial pre-calibration is performed. Since the output current is zero, for this condition the estimated current is equal to that of the offset. In the following step the obtained offset is dynamically taken into account and cancelled by *Calibration Logic* (Fig. 1). This allows the estimator to be used in digital controllers where the dead-time is dynamically changed for improving converter efficiency [21]. It should be noted that in many applications no additional hardware is needed for disconnecting the load. Modern supplies usually have a power good signal, allowing the loads to be connected only after the nominal voltage conditions are established.

The deviation of the input voltage at the beginning of the switching cycle, caused by a pulsating input current is illustrated in Fig. 5. This deviation exists even when a fairly good input filter is used. It results in an effectively smaller average input converter voltage when the high-side MOSFET is turned on. For large loads, this voltage drop causes a large estimation error. To compensate for it, the position of the

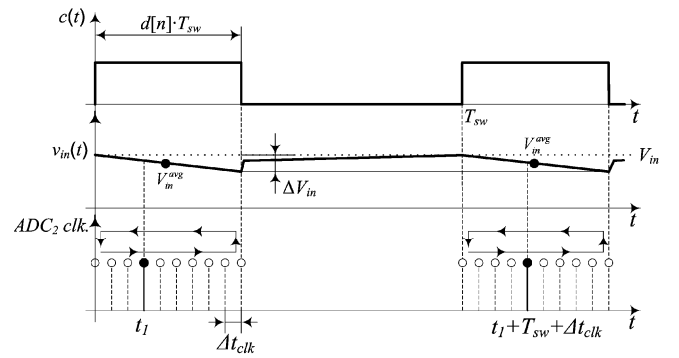


Fig. 5. Variation of the input voltage $v_{in}(t)$ during a switching cycle and proposed rotating sampling scheme

sampling instant is constantly rotated and an average value of the samples is taken. In this way the actual value of the average input voltage during the transistor on time is obtained and the error in estimation is eliminated.

It should be noted that the shown implementation of the estimator does not require a powerful fast sampling ADC for input voltage measurement. To obtain the input voltage, the existing ADC for the output voltage measurement can be time shared or, as shown here, a slow ADC with a sampling rate much lower than the switching frequency can be utilized.

IV. EXPERIMENTAL SYSTEMS AND RESULTS

An experimental system was built based on the diagrams shown in Figs. 1 and 3. The power stage is a 15-W, 6.5 V-to-1.5 V buck converter. The estimator and controller are implemented with an FPGA board and commercially available ADCs sampling the output and input voltages. For demonstration purpose, the test current sink was set to produce a 2 A current step (i.e. 20 % of the converter rated current) for 300 μ s every 300 ms, taking only 0.1% of the total operating time and resulting in average power dissipation of 3 mW only. This value can be further reduced if the time interval between

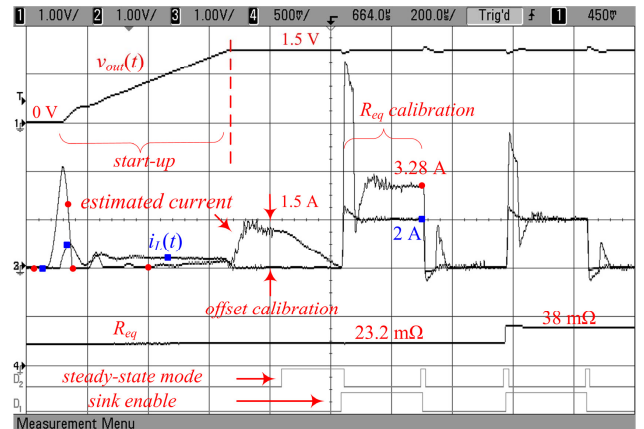


Fig. 6. System operation after the start-up – Ch1: Output converter voltage (1V/div); Ch2: actual averaged inductor current $i_L(t)$ – 2 A/V; Ch3: estimated steady-state current i_{steady} – 2 A/V; D1-D2- sink enable and steady-state mode; Time scale is 200 μ s/div.

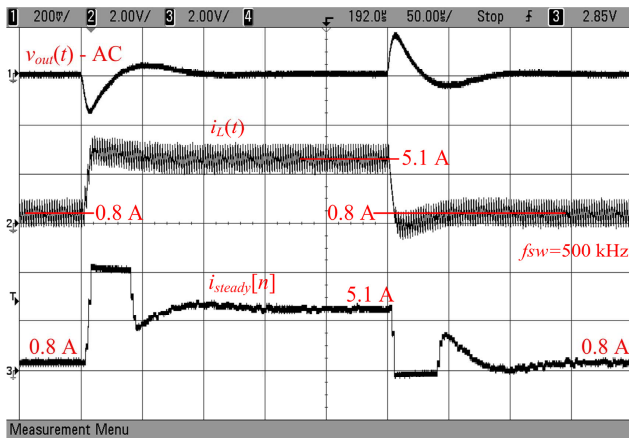


Fig.7. System operation during the load transient – Ch1: Output converter voltage (200mV/div); Ch2: actual inductor current $i_L(t)$ – 2 A/V; Ch3: estimated steady-state current i_{steady} – 2 A/V; Time scale is 50 μ s/div.

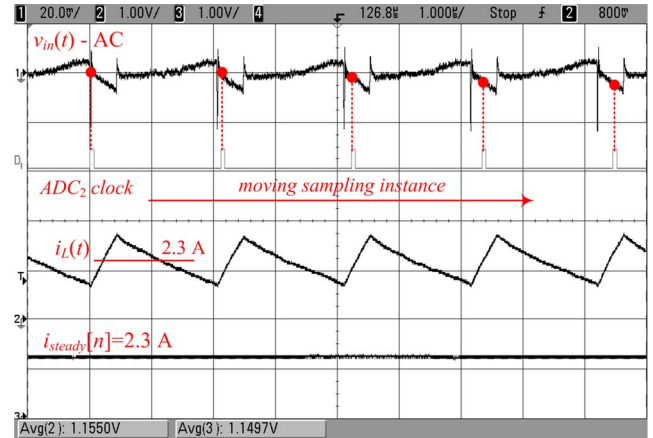


Fig.8. System operation in the steady state – Ch1: input converter voltage (20mV/div); Ch2: actual inductor current $i_L(t)$ – 2 A/V; Ch3: estimated steady-state current i_{steady} – 2 A/V; Time scale is 1 μ s/div.

two calibration steps is increased. To observe the estimated current $i_{steady}[n]$ and R_{eq} , their digital equivalents, produced by the estimator, are fed to digital-to-analog converters and the resulting analog values are measured.

A. Current Estimation

Fig. 6 illustrates system operation shortly after start-up. First, the current offset of 1.5 A, due to the dead-time action, is eliminated. In the next step, a 2 A current step is introduced and a mismatch between the initially assumed R_{eq} and the actual value is compensated (the value of 23.2 m Ω is corrected to 38 m Ω). Consequently, the accuracy of the current estimation is improved. Initial value of 3.28 A is corrected to 2 A. Figs. 7 and 8 verify proper estimation during regular converter operation. It can be seen that the estimator accurately tracks load current changes.

Fig. 8 also shows the *rotating* sampling scheme applied for the correction of the input voltage variation, as described in Section III. The input voltage of the converter is sampled at

the switching frequency and every cycle the sampling instant is shifted by a fraction of the switching period. It should be noted that the same rotating scheme can be implemented with under sampling to minimize hardware requirements for the ADC.

B. Temperature Monitoring and Overheating Protection

Figs. 9 and 10 verify proper operation of the temperature estimator/protection block from Fig. 1. To test its operation, the converter power MOSFETs are intentionally heated up. As it can be seen from Fig.9, this results in an increase of R_{eq} (see Fig.10) above the threshold resistance R_{thresh} , and triggering the overheating protection signal.

C. Accuracy of Current and Temperature Estimation

The accuracy of the current estimation is assessed by changing the load current and comparing it to the estimated value. Fig. 11, shows that a fairly good estimate is obtained. For the full load, the error of the estimation is less than 2% while for 90% of the full load it is about 5.3%. At lighter loads

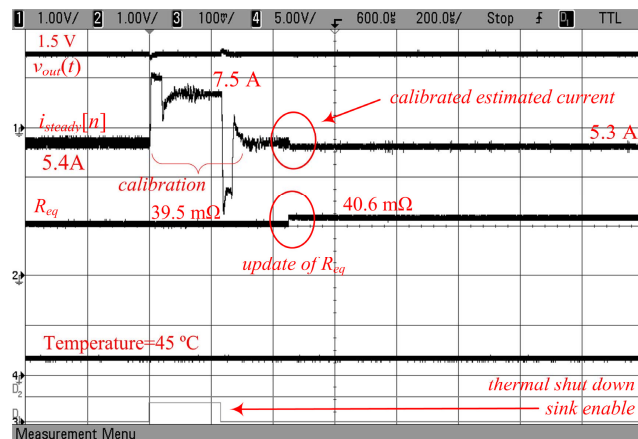


Fig.9. Thermal protection is not active – Ch1: Output converter voltage (1V/div); Ch2: estimated steady-state current i_{steady} – 2 A/V; Ch3: estimated R_{eq} – 10mOhms/102.4mV; Ch4: MOSFET temperature – 25 $^{\circ}$ C/V; D1-D2- sink enable and thermal shut down. Time scale is 200 μ s/div.

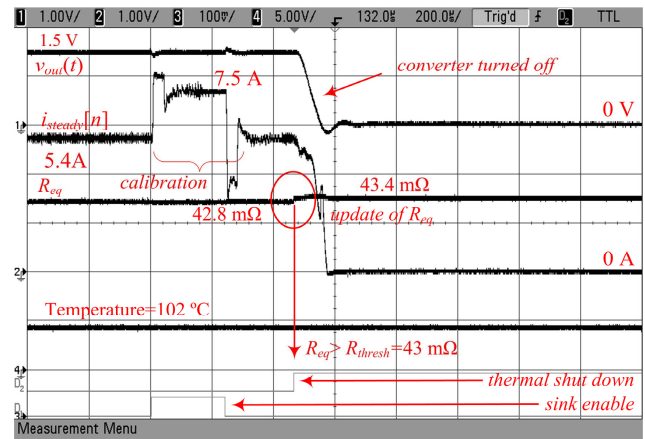


Fig.10. Thermal protection is activated at 102 $^{\circ}$ C and **converter is turned off** – Ch1: Output converter voltage (1V/div); Ch2: estimated steady-state current i_{steady} – 2 A/V; Ch3: estimated R_{eq} – 10mOhms/102.4mV; Ch4: MOSFET temperature – 25 $^{\circ}$ C/V; D1-D2- sink enable and thermal shut down. Time scale is 200 μ s/div.

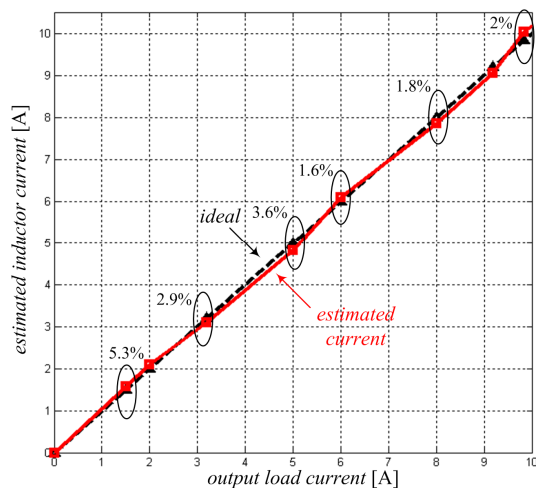


Fig. 11. Estimated inductor current versus the output load current

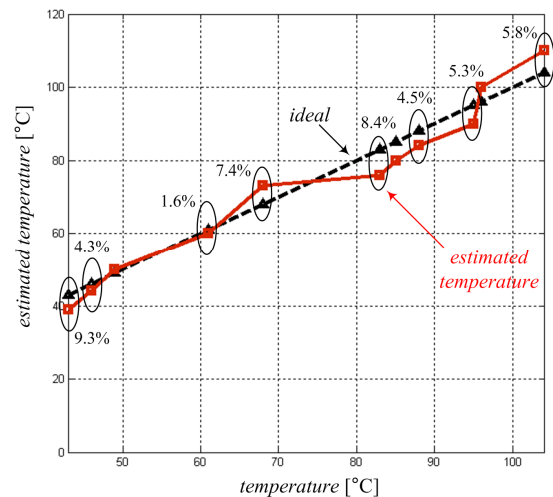


Fig. 12. Estimated temperature versus sensor temperature

the error increases due to quantization effects.

Fig. 12 shows results of the temperature estimation. It can be seen that the absolute error of the temperature estimation is limited to ± 7 °C while the relative error is less than 10 %. The precision of this measurement depends on the size of the look-up tables and the accuracy of data stored in the estimator look-up tables.

V. CONCLUSION

This paper introduces a combined current and temperature estimator, suitable for single-chip integration with low-power digitally controlled switch-mode power supplies. The system utilizes information from the duty ratio value and a test current sink to accurately determine load current and equivalent resistance R_{eq} of the converter circuit. Based on the estimated R_{eq} , the temperature of the switching components is roughly estimated. The negative effects of the dead-time circuit and the input voltage variation on the measurement accuracy are eliminated by the initial offset cancellation and a rotating sampling scheme. Operation of the system is successfully verified with an experimental prototype.

REFERENCES

- [1] J. Xiao, A. V. Peterchev, J. Zhang, and S. R. Sanders, "A 4- μ A Quiescent-Current Dual-Mode Digitally Controlled Buck Converter IC for Cellular Phone Applications," *IEEE Journal of Solid-State Circuits*, vol. 39, pp. 2342–2348, Dec. 2004.
- [2] N. Rahman, A. Parayandeh, K. Wang, and A. Prodić, "Multimode digital SMPS controller IC for low-power management," in *Proc. IEEE International Symposium on Circuits and Systems*, 2006, pp. 5327 – 5330.
- [3] O. Trescases, W. T. Ng, H. Nishio, M. Edo, T. Kawashima, "A Digitally Controlled DC-DC Converter Module with a Segmented Output Stage for Optimized Efficiency," in *Proc. IEEE Power Semiconductor Devices and ICs*, 2006, pp. 1 – 4.
- [4] Data Sheet, TPS 62300, 500-mA, 3-MHz Step-Down Converter, Texas Instruments Inc.
- [5] Data Sheet, MAX 85600, 500 mA, 4-MHz Step-Down DC-DC Converter, Maxim.
- [6] H. Forghani-zadeh and G. Rincón-Mora, "Current sensing techniques for DC-DC converters," in *Proc. IEEE MWSCAS*, Aug. 2002, pp. 577– 580.
- [7] P. Givelin and M. Bafleur, "On-chip over-current and open-load detection for a power MOS high-side switch: a CMOS current-source approach," in *Proc. European Conf. Power Electronics and Applications*, 1993, pp. 197–200.
- [8] S. Yuvarajan and L. Wang, "Power conversion and control using a current-sensing MOSFET," in *Proc. Midwest Symp. Circuits and Systems (MWSCAS)*, 1992, pp. 166–169.
- [9] J. Chen, J. Su, H. Lin, C. Chang, Y. Lee, T. Chen, H. Wang, K. Chang, and P. Lin, "Integrated current sensing circuits suitable for step-down DC-DC converters," *IEE Electron. Letters*, pp. 200–201, Feb. 2004.
- [10] C. Lee and P. Mok, "A monolithic current-mode CMOS DC-DC converter with on-chip current-sensing technique," *IEEE Journal of Solid-State Circuits*, vol. 39, no. 1, pp. 3–14, Jan. 2004.
- [11] E. Dallago, M. Passoni, and G. Sassone, "Lossless current sensing in low-voltage high-current DC/DC modular supplies," *IEEE Trans. Ind. Electron.*, vol. 47, pp. 1249 – 1252, Dec. 2000.
- [12] P. Midya, P. T. Krein, and M. F. Greuel, "Sensorless current mode control—an observer-based technique for DC-DC converters," *IEEE Trans. Power Electron.*, vol. 16, pp. 522 – 526, Jul. 2001.
- [13] H. P. Forghani-zadeh and G. A. Rincón-Mora, "An accurate, continuous, and lossless self-learning CMOS current-sensing scheme for inductor-based DC-DC converters," *Proc. IEEE Journal of Solid-State Circuits*, vol. 42, pp. 665 – 679, Mar. 2007.
- [14] G. Garcea, S. Saggini, D. Zambotti, and M. Ghioni, "Digital auto-tuning system for inductor current sensing in VRM applications," in *Proc. IEEE Applied Power Electronics Conf.*, 2006, pp. 493 – 498.
- [15] A. Kelly and K. Rinne, "Sensorless current-mode control of a digital dead-beat DC-DC converter," in *Proc. IEEE Applied Power Electronics Conf.*, 2004, pp. 1790 – 1795.
- [16] O. Trescases, A. Parayandeh, A. Prodić, and W. T. Ng, "Sensorless digital peak current controller for low-power DC-DC SMPS based on a bi-directional delay line," in *Proc. IEEE Power Electronics Specialist Conf.*, Jun. 2007, pp. 1670 – 1676.
- [17] L. Hua and S. Luo, "Design considerations of time constant mismatch problem for inductor DCR current sensing method," in *Proc. IEEE Applied Power Electronics Conf.*, 2006, pp. 1368 – 1374.
- [18] A. Prodić and D. Maksimović, "Digital PWM controller and current estimator for a low-power switching converter," in *Proc. IEEE Computers in Power Electronics Conf.*, 2000, pp. 123 – 128.
- [19] Z. Lukić, Z. Zhao, S. M. Ahsanuzzaman, A. Prodić, "Self-tuning digital current estimator for low-power switching converters," in *Proc. IEEE Applied Power Electronics Conf.*, 2008.
- [20] R. W. Erickson and D. Maksimović, *Fundamentals of Power Electronics*, 2nd edition. Boston, MA: Kluwer 2000.
- [21] V. Yousefzadeh, D. Maksimović, "Sensorless Optimization of Dead Times in DC-DC Converters With Synchronous Rectifiers," *IEEE Trans. Power Electron.*, vol. 21, pp. 994 – 1002, Jul. 2006.